JOC Article

Mechanism of Novel Consecutive Rearrangements of Cyclobutene-Fused Diphenylhomobenzoquinones Catalyzed by Lewis Acids

Takuya Koizumi, Eiko Mochizuki, Ken Kokubo, and Takumi Oshima*

Department of Materials Chemistry, Graduate School of Engineering, Osaka University, Toyonaka, Osaka 560-0043, Japan

oshima@ch.wani.osaka-u.ac.jp

Received December 17, 2003

Lewis acid catalyzed rearrangements of highly strained [2 + 2] photoadducts **1a**−**d** of diphenylhomobenzoquinone with various acetylenes were investigated under the influence of $AlCl_3$, $SnCl_4$, BF_3, and $TiCl_4$. With the relief of steric strain, these tricyclo[5.2.0.$0^{3,5}$]non-8-ene-2,6-diones underwent the three steps of consecutive skeletal transformations. The first step was the two-way cyclobutene ring-cleavage reaction with a Wagner−Meerwein vinyl migration to either Lewis acid activated carbonyl function. This process virtually occurred under the anchimeric assistance of the *endo*-phenyl ring to give, after proton transfer, the phenylene-bridged tetracyclic keto alcohols **2** and **3**, respectively. The next step was the acid-induced cyclopropane ring cleavage of only **3** to lead to bicyclic diones **4** via a following stereoselective proton transfer. The last one involved a Michael-type intramolecular cyclization of **4** accompanied by a proton transfer to afford thermodynamically less stable tricyclic diones **5**α which epimerized to **5**β only by $TiCl_4$. The factors that control the selectivity and the reactivity of these tandem reactions were addressed on the basis of the X-ray crystal analyses as well as the PM3 calculations. It was found the present Lewis acid-catalyzed rearrangements were very dependent on the substituents of **1a**−**d** and the nature of the Lewis acids.

Introduction

The rearrangement reaction, which breaks carbon−carbon bonds as well as constructs them, is one of the most sophisticated and powerful means for the construction of a variety of new carbon skeletons. Investigation of such structural transformations has been the subject of considerable interest from synthetic and mechanistic viewpoints, and a great number of reports and reviews have been published.[1] Acid-catalyzed rearrangements, which involve the activation of incorporated carbonyl function(s), are interesting because a large fraction of chemical reactions and an even larger fraction of biochemical reactions involve the C═O group.[2] Reactions of this kind show a variety of fundamental features of cationic organic reactions. In particular, polycyclic ketones possessing high strain energy are intriguing compounds on account of a great capability of suffering a rearrangement in the presence of an acid or a Lewis acid catalyst. In addition, the product polycyclic compounds are considered to have a unique carbon skeleton, which is rather difficult or impossible to produce by conventional methods. In this connection, we have designed and synthesized the highly strained tricyclic diones from the [2 + 2] photocycloaddition of alkynes with diphenylhomobenzoquinone.[3] These photoadducts **1a**−**d** (Chart 1) are expected to show some novel ring-cleavage events because of the feasible relief of cyclobutene and cyclopropane ring strain. Indeed, a preliminary acid-promoted rearrangement of **1a** has revealed that the reaction proceeds through a tandem skeletal transformation

(1) (a) Murray, A. W. Molecular Rearrangements. In *Organic Reaction Mechanisms*; Knipe, A. C., Watts, W. F., Eds.; John Wiley & Sons: Chichester, 2003; Chapter 15, pp 487−615. (b) Smith, M. B.; March, J. Rearrangements. In *March's Advanced Organic Chemistry*, 5th ed.; John Wiley & Sons: New York, 2001; Chapter 18, pp 1377−1505. (c) Harwood; L. M. *Polar Rearrangements*; Oxford University Press Inc.: New York, 1992. (d) Ho., T.-L. Rearrangements and Fragmentations. In *Tandem Organic Reactions*; John Wiley & Sons: New York, 1992; Chapter 13, pp 361−397. (e) Mundy, B. P.; Ellerd, M. G. *Name Reactions and Reagents in Organic Synthesis*; Wiley: New York, 1988. (f) Lowry, T. H.; Richardson, K. S. Intermolecular Cationic Rearrangements. In *Mechanism and Theory in Organic Chemistry*, 3rd ed.; Harper Collins: New York, 1987; Chapter 5, pp 425−515. (g) Hendrickson, J. B. *J. Am. Chem. Soc.* **1986**, *108*, 6748. (h) Ahlberg, P.; Jonsall, G.; Engdahl, C. Degenerate Carbocation Rearrangements. In *Advances in Physical Organic Chemistry*; Gold, V., Bethell, D., Eds.; Academic Press: London, 1983; Vol. 19, pp 223−379. (i) Mayo, P. de *Rearrangements in Ground and Excited States*; Academic Press: London, 1980; Vols. 1−3. (j) Spangler, C. W. *Chem. Rev.* **1976**, *76*, 187.

(2) (a) Cargili, R. K.; Pond, D. M.; Le Grand, S. O. *J. Org. Chem.* **1970**, *36*, 1423. (b) Fitjer, L.; Majewski, M.; Kanschik, A. *Tetrahedron Lett.* **1988**, *29*, 1263. (c) Stork, G.; Grieco, P. A. *J. Am. Chem. Soc.* **1969**, *91*, 2407. (d) Hantawong, K.; Murphy, W. S.; Boyd, D. R.; Ferguson, G.; Parvez, M. *J. Chem. Soc., Perkin Trans. 2* **1985**, 1577. (e) Duc, D. K. M.; Fetizon, M.; Lazare, S. *Chem. Commun.* **1975**, 282. (f) Kakiuchi, K.; Ue, M.; Tsukahara, H.; Shimizu, T.; Miyao, T.; Tobe, Y.; Odaira, Y. *J. Am. Chem. Soc.* **1989**, *111*, 3707. (g) Hirao, K.; Tanigichi, M.; Yonemitsu, O.; Flippen, J. L.; Witkop, B. *J. Am. Chem. Soc.* **1979**, *101*, 408. (h) Ogino, T.; Awano, K.; Fukazawa, Y. *J. Chem. Soc., Perkin Trans. 2* **1990**, 1735. (i) SindlerB. B.; Kirk, T. C. *J. Am. Chem. Soc.* **1983**, *105*, 2364. (j) Denmark, S. E.; Hite, G. A. *Helv. Chim. Acta* **1988**, *71*, 195.

(3) Kokubo, K.; Yamaguchi, H.; Kawamoto, T.; Oshima, T. *J. Am. Chem. Soc.* **2002**, *124*, 8912.

10.1021/jo035830k CCC: $27.50
Published on Web 06/15/2004

CHART 1

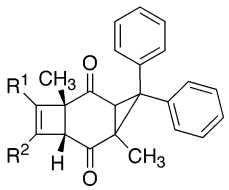

1

	R^1	R^2
a:	Ph	Me
b:	Ph	Ph
c:	*n*-Bu	H
d:	Et	Et

involving the cleavage of the two strained cyclobutene and cyclopropane rings.[4] Herein, we extended the investigation to the other [2 + 2] cycloadducts **1b**−**d** of various acetylenes with the homobenzoquinone. The sequential steps of the reactions were also controlled by the acetylene substituents and the nature of the Lewis acids used. On the basis of the detailed X-ray structural analyses as well as PM3 calculations of the products and the Lewis acid−carbonyl copmlexes, we intended to explore the steric and electronic factors that govern the selectivity and reactivity of the acid-catalyzed rearrangements of these tricyclic diones.

Results and Discussion

Synthesis and Structural Characteristics of the Photoadducts (1a−d) of Alkynes and Homobenzoquinone. Cyclobutene-fused homobenzoquinones **1a**−**d** were prepared by the [2 + 2] photocycloadditions of various alkynes (diphenylacetylene, 1-phenyl-1-propyne, 3-hexyne, and 1-hexyne) to the homobenzoquinone.[3] The regiochemistry of photoadditions for the unsymmetrical alkynes was governed by the relative stability of the 1,4-biradical intermediates.[3] The head-to-head (HH) type adducts were preferentially obtained in preference to the head-to-tail (HT) ones (>10:1). Due to the poor yields of HT adducts, we carried out the Lewis acid catalyzed rearrangements only for the major HH adducts.

As shown in Figure 1, the whole structures of the major adducts were elucidated by the X-ray crystal structural analysis of **1a** as *cis-transoid-cis*, representing the *anti*-addition of alkynes with respect to the cyclopropane ring of homobenzoquinone. It was also found that the original quinone ring adopts a pseudo-boat conformation.[5] Such a slight-upward deformation of the parent quinone frame causes an appreciable pseudoaxial flipping of the conjunct planar cyclobutene ring.[6] Namely, both the cleavable cyclobutene σ bonds lie approximately parallel to the axes of the vacant carbonyl π^* orbital. This may enhance the $\sigma-\pi^*$ interaction which will accelerate cyclobutene ring cleavage followed by the 1,2-vinyl migration.[7] It is also noted that the *endo*-phenyl ring overhangs above the

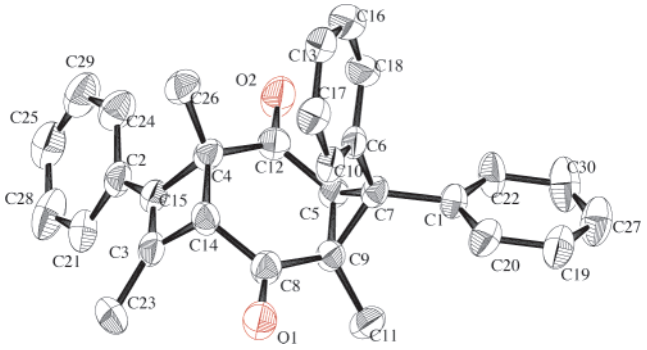

FIGURE 1. ORTEP drawing of tricyclic endione **1a**.

quinone plane and hence is capable of suitably donating the π-electron cloud to the developing positive carbon atom of the quinone frame. This type of π-electron participation was found to be very important in the present Lewis acid catalyzed rearrangements as in S_N2 reactions.[8] As a result, the geometrical structure of **1a** can take an advantage of σ- and π-anchimeric assistance in the present acid-catalyzed rearrangements (vide infra).

General Feature of Acid-Catalyzed Rearrangements of 1a−d. The acid-catalyzed rearrangements of **1** (30 mM) with 3 equiv excess of $AlCl_3$, $SnCl_4$, BF_3, and $TiCl_4$ were carried out in $CDCl_3$ at room temperature according to the procedure described previously.[4] As shown in Scheme 1, the general feature of these sequential reactions consists of the three steps of prominent skeletal transformations: (1) the two partitioning 1, 2-vinyl migration associated with the phenylene annulation to give the corresponding two tetracyclic keto-alcohols **2** and **3**, (2) the subsequent cyclopropane ring cleavage of **3** to afford the bicyclic diones **4**, and (3) the Michael-type intramolecular cyclization to yield tricyclic diones **5**. All steps accompanied the proton transfer or migration. For convenience, we call the partitioning ring cleavage leading to **2** (via the secondary carbocation intermediate **I**) and **3** (via the tertiary carbocation intermediate **II**) paths A and B, respectively.

Here, it is noteworthy that **2** and **3** are mirror images of each other with respect to only the cage skeleton. Strangely, however, compounds **2** did not undergo the subsequent cyclopropane ring cleavage, but the **3** rearranged to the bicyclic diones **4**. The details of the reactivity difference between **2** and **3** will be discussed in a later section. The resulting bicyclic diones **4** were further transformed into the tricyclic diones **5** via the acid-mediated cyclization except for **4b** ($R^1 = R^2 = Ph$). In addition, only the reaction of **1b** yielded a certain amount of concomitant epimer **4b**β. Furthermore, only $TiCl_4$ caused the epimerization of **5a**α and **5c**α into the respective β-isomers. The intricate structures of these products were determined by X-ray structural analyses along with ^1H and ^{13}C NMR spectra. The product distributions for the Lewis acid-catalyzed reactions of **1a**−**d** were collected in Table 1.

(4) Kokubo, K.; Koizumi, T.; Yamaguchi, H.; Oshima, T. *Tetrahedron Lett.* **2001**, *42*, 5025.

(5) The pseudo-boat conformation can be anticipated by the dihedral angle (θ) of 172.3° for the linkage of O(1)−C(8)−C(14)−C(4) and −178.7° for O(2)−C(12)−C(4)−C(14), respectively; see Figure 1.

(6) This is reflected in the smaller dihedral angle (θ) of 109.2° for the C(15)−C(4)−C(14)−C(8) linkage involving cyclobutene σ-bond as compared to 135.3° for the C(8)−C(14)−C(4)−C(26) linkage involving the quinone methyl substituent; see Figure 1.

(7) (a) Kirby, A. J. *Stereoelectronic Effects*; Oxford University Press, Inc.: New York, 1966. (b) Deslongchamps, P. *Stereoelectronic Effects in Organic Chemistry*; Pergamon Press: Oxford, 1983.

(8) (a) Brown, H. C.; Liu, K.-T. *J. Am. Chem. Soc.* **1969**, *91*, 5909. (b) Dirlam, P. J.; Winstein, S. *J. Am. Chem. Soc.* **1969**, *91*, 5905. (c) Gassman, P. G.; Fentiman, A. F., Jr. *J. Am. Chem. Soc.* **1970**, *92*, 2549. (d) Reters, E. N.; Brown, H. C. *J. Am. Chem. Soc.* **1973**, *95*, 2398. (e) Brown, H. C.; Ravindranathan, M.; Peters, E. N. *J. Am. Chem. Soc.* **1974**, *96*, 7351. (f) Brown, H. C.; Ikegami, S.; Liy, K.-T.; Tritle, G. L. *J. Am. Chem. Soc.* **1976**, *98*, 2531.

SCHEME 1

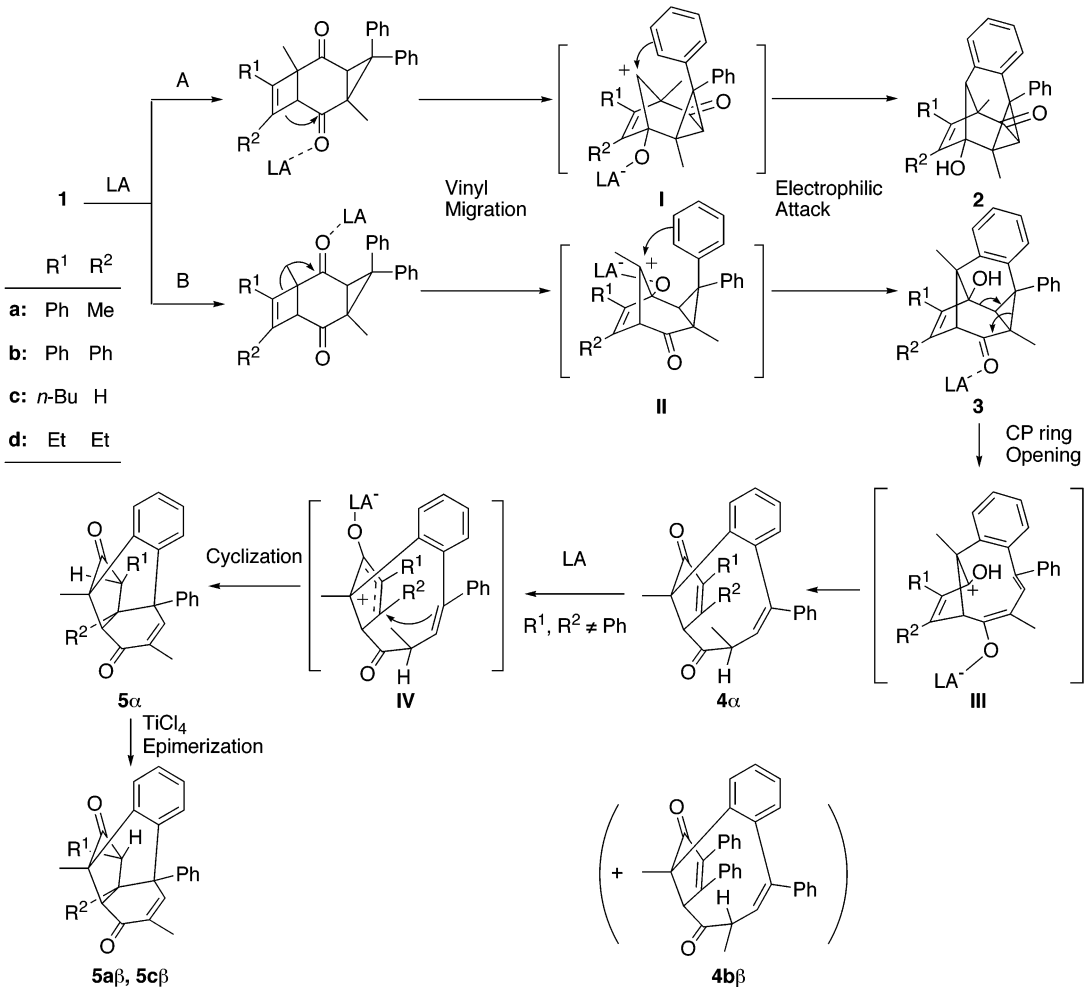

TABLE 1. Product Distributions in Lewis Acid Catalyzed Rearrangement of 1a−d (30 mM) in $CDCl_3$ at 25 (±2) °C

					yield[a,b]/%					
					path A[c]	path B[c]				
entry	substrate	Lewis acid[d]	time/h	conv/%[b]	**2**	**3**	**4α**	**4β**	**5α**	**5β**
1	**1a**	$AlCl_3$[e]	14	84	27		31		42	
2	**1a**	$AlCl_3$	60	94	28		15		57	
3	**1a**	$SnCl_4$	2	98	22		7		70	
4	**1a**	BF_3	2	100	42 (±2)[f,g]				58 (±2)[f,g]	
5	**1a**	$TiCl_4$	0.2	100	6				88	6
6	**1a**	$TiCl_4$	20	100	7				33	60
7	**1b**	$AlCl_3$[e]	70	46[h]		4	54	32		
8	**1b**	$SnCl_4$	20	64		79	18	3		
9	**1b**	$SnCl_4$	70	100		16	72	11		
10	**1b**	BF_3	20	87		21	51	25		
11	**1b**	BF_3	70	100		2	63	35		
12	**1b**	$TiCl_4$	0.1	100		∼100[i]				
13	**1c**	$SnCl_4$	70	100	21				79	
14	**1c**	BF_3	70	100	22				78	
15	**1c**	$TiCl_4$	1	100	25				75	
16	**1c**	$TiCl_4$	70	100	26				10	64
17	**1d**	$SnCl_4$	70	100	6				93	
18	**1d**	BF_3	70	100[j]	15				79	
19	**1d**	$TiCl_4$	70	100	-				∼100	

[a] Based on consumed **1a**−**d**. [b] Determined by ^1H NMR. [c] Products via path A and path B, respectively; see Scheme 1. [d] 3 equiv of Lewis acid was used with respect to **1a**−**d**. [e] In $CHCl_3$. [f] Average of two experiments. [g] Unchanged even on standing for 40 h. [h] Unidentified product was detected in 10%. [i] Unchanged even on standing for 200 h. [j] Unidentified product was detected in 6%.

Because of the fusion of highly strained cyclobutene and cyclopropane rings,[9] rearrangements of **1** are considered to exhibit the step-by-step energy drops. We calculated the enthalpies (ΔH_f) of formation for the isolated and expected products **2**−**5** as well as **1** by the MOPAC PM3 method (Table 2). The relief of cyclobutene ring strain (29 kcal mol^{-1}) is reflected in the large enthalpy drop in the range of 21−29 kcal mol^{-1} for the

TABLE 2. Heat of Formation (ΔH_f) of Consecutive Rearrangement Products from 1a−d[a]

	ΔH_f/kcal mol^{-1}						
substrate	**1**	**2**	**3**	**4α**	***4β***	**5α**	***5β***
1a	58.5	32.9	(36.3)	33.3	(32.3)	30.2	22.2
1b	94.2	(69.6)	71.5	69.1	68.9	(74.2)	(62.9)
1c	21.4	−8.2	(−4.8)	(−6.1)	(−7.2)	−21.0	−26.1
1d	17.1	−10.8	(−4.3)	(−10.8)	(−12.5)	−16.4	(−18.4)

[a] Calculated by the MOPAC PM3 method. The values in parentheses were calculated for the possible products.

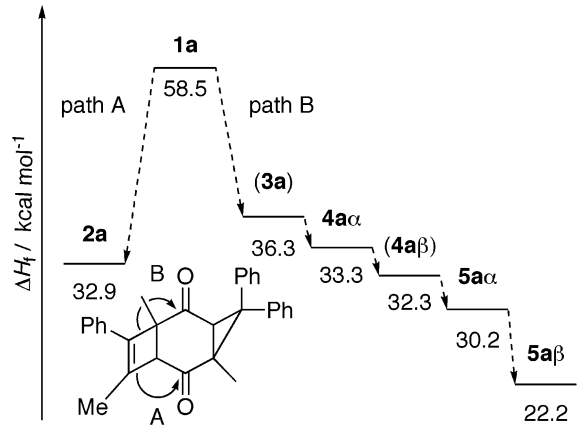

FIGURE 2. Energy level diagram for the consecutive rearrangements of **1a**. Heat of formation (ΔH_f) was calculated by the MOPAC PM3 method.

first transformation **1** → **2** or **3**.[9] The sequential progress of path B route for **1a** is also envisaged in the decreasing ΔH_f values in the order of **1a** > **3a** > **4a**α > **4a***β* > **5a**α > **5a***β* (Figure 2). Here, the suffixes α and *β* represent the epimer of each other.

In this paper, we have paid special attention to the substituent effects on each step of the tandem skeletal rearrangements of **1a**−**d** as well as on the Lewis acid dependency of these processes. In the following section, we will focus on the reaction feature of each step of rearrangements in comparison with **1a** as a reference substrate.

Reaction of 1-Phenyl-1-propyne Adduct 1a. As seen in Table 1, the reaction of title compound **1a** with $AlCl_3$ (3 equiv) for 14 h gave a mixture of tetracyclic keto alcohol **2a** (27%), bicyclic dione **4a**α (31), and tricyclic dione **5a**α (42), respectively, upon 84% conversion (entry 1). The extended reaction time (60 h) caused an increase of **5a**α by 15% and a decrease of **4a**α by almost the same extent (16%) (entry 2), although the relative amount of **2a** was essentially unchanged (27−28%). This result apparently indicates that **2a** was formed via a different pathway from that leading to **4a**α and also that the **4a**α was further transformed into **5a**α. Since **1a** has two carbonyl groups capable of binding Lewis acid, the two regiochemical modes of cyclobutene bond cleavage are likely to lead to the different tetracyclic keto alcohols **2** (path A) and **3** (path B), respectively (Scheme 1). Accordingly, the formation of **4a**α can be rationalized by the acid-mediated cyclopropane ring-cleavage of labile product **3a**. This process is accomplished by the simultaneous fission of the cyclopropane-connecting inner bond as well as the proton transfer. Similarly, the $SnCl_4$-catalyzed reaction of **1a** provided the same products **2a**, **4a**α, and **5a**α in roughly comparable distributions, although the transformation of **4a**α into 5**a**α was far more accelerated compared with the $AlCl_3$ reaction (entry 3). On the other hand, BF_3- and $TiCl_4$-catalyzed reaction resulted in the complete conversion of **1a** and the rapid transformation **4a**α → **5a**α within 2 h (entries 4 and 5). In the BF_3 reaction, product **2a** was relatively increased (42%) and the product mixture with **5a**α (58%) remained unchanged even on further 40 h standing. However, the $TiCl_4$ reaction, which gave a considerable amount of **5a**α (88%) along with low yields of **2a** (6%) and **5a**α (6%) on 0.2 h treatment, gradually caused the epimerization of **5a**α into the more stable **5a***β* (60%) on further 20 h standing (entries 5 and 6).

Considering the above product distributions and the stereochemical consequences, several questions have emerged as follows.

(1) What factors determine the ratio of path A (**2a**) to path B products (as summation of **4a**α, **5a**α, and *β*)?

(2) Why does **2a** resist the subsequent cyclopropane ring cleavage?

(3) Why does this ring cleavage of **3a** exclusively provide the α-epimer of **4a** after proton transfer?

(4) Why does the Michael-type cyclization of **4a**α lead to the less stable epimer **5a**α?

We wish to approach the first question by resorting to the two principal factors: (a) Lewis acid binding affinity (i.e., binding constant *K*) of each carbonyl function and (b) the rate constant *k* for the cyclobutene ring cleavage of the Lewis acid activated complex (eq 1). Consequently, the path B/path A ratio can be represented by eq 2.

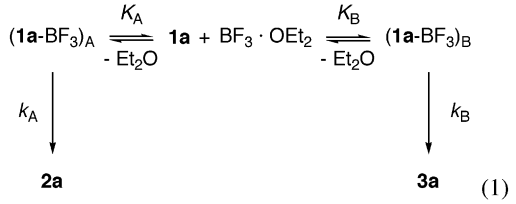

$$\text{path B / path A} = k_B K_B / k_A K_A \qquad (2)$$

The *K* depends on the steric environments around the carbonyl groups of **1a** as well as on the electron-accepting ability of the Lewis acids. So, we have to consider the structure of carbonyl−Lewis acid complexes. A survey of the Cambridge Structural Database (CSD) demonstrated that the central atom (M) of Lewis acids lies in the direction of the carbonyl lone pair without larger distortion away from the best plane of the carbonyl group. The average values of C−O−M bond angles (φ) and the O−M bond length (*r*), obtained from CSD, are 116 ± 4° and 1.58 Å (for BF_3), 136 ± 4° and 1.88 Å (for $AlCl_3$), 125 ± 12° and 2.14 Å (for $TiCl_4$), and 127 ± 10° and 2.3 Å (for $SnCl_4$), respectively. [10]

Accordingly, such carbonyl−Lewis acid complexation of **1a** seems to preferentially occur at the least or less congested lone pair electrons a_1 and b_2 because of the substitution of hydrogen atoms (H^a and H^b) (Chart 2).

(9) The ring strain in cyclobutene is 29 kcal mol^{-1} (Schleyer, P. v. R.; Williams, J. E., Jr.; Blanchard, K. R. *J. Am. Chem. Soc.* **1970**, *92*, 2377) and that in cyclopropane is 27 kcal mol^{-1} (Liebman, J. E.; Greenberg, A. *Chem. Rev.* **1976**, *76*, 311).

CHART 2

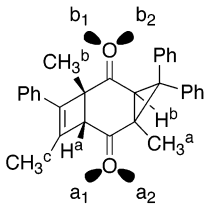

In contrast, the coordination at the a_2 and b_1 sites may be unfavorable by the adjacent α-methyl groups (CH_3^a and CH_3^b). To ensure the probable binding site of Lewis acid, we have examined the ^{1}H NMR spectral changes of **1a** (30 mM) with increasing amounts of BF_3·OEt_2 (0.5−3 equiv) in $CDCl_3$. As shown in Figure 3, **1a** exhibited the increasing low-field shifts of these diagnostic protons with increasing equivalency of Lewis acid, although the remote vinyl-substituted CH_3^c was essentially unsusceptible. The H^b proton demonstrated the largest increment in the low-field shift with increasing Lewis acid, while the H^a shift is rather modest and asymptotic. On the other hand, both the methyl groups CH_3^a and CH_3^b showed the very similar profiles with weaker low-field chemical shifts. A straightforward understanding of Figure 3 is that BF_3 tends to bind predominantly at the lone pair b_2 and preferentially induces the path B cyclobutene ring cleavage. In fact, the path B/path A ratio of 1.4 was observed in the presence of excess BF_3 (Table 1, entry 4).

To assess the binding affinities of the relevant four lone pairs a_1−b_2 of **1a**−**d**, the PM3 calculations were performed for the complexation with BF_3 and $AlCl_3$ (Table 3).[11] Except for the combination of **1a** and BF_3 which provided −2.9 kcal mol^{-1} for $\Delta\Delta H_f(a_1-b_2)$, the most cases exhibited the favorable binding to the b_2 lone pair by 0.1−2.6 kcal mol^{-1}, in conformity with the selective occurrence of path B process (Table 1). However, the very small difference in ΔH_f implies no substantial drift to the either side in the equilibration (eq 1).

As for the rate constant k, we first need to know whether a stepwise or a concerted mechanism is applied for the formation of keto alcohols **2** and **3**. If the reaction proceeds via the stepwise manner, the k_B becomes larger than the k_A because of the greater stabilization of tertiary carbocation intermediate **II** than the secondary one **I** (Scheme 1). By contrast, the concerted pathway would realize the larger k_A as compared with k_B because the cyclobutene ring cleavage followed by the concerted *endo*-phenyl annulation is apt to occur via the less crowded path A transition state. As shown in Table 1, the fact that the path B prevails 1.4 times (for BF_3) more than the path A rather suggests the intervention of the carbocation intermediate or the positively charged transition state. To examine the possible appearance of carbocation intermediates, we carried out the trapping experiment using 20 equiv of CH_3OH with respect to **1a** in the presence of 3 equiv of BF_3. The reaction provided no methanol adducts but performed the same product distribution, as did the methanol-free reaction. However, this failure cannot thoroughly rule out the possibility that the generated ionic intermediates such as **I** and **II** suffered very rapid annulation by *endo*-phenyl group. Consequently, it was found that the path B/path A ratios (which are equivalent to k_BK_B/k_AK_A ratios) varied in the range of 1.4−16 on going from BF_3 to $TiCl_4$ (Table 1).

The second question on the Lewis acid persistency of keto alcohol **2a** is also rationalized by considering the unfavorable steric effects on the Lewis acid binding to the carbonyl function of **2a**. As mentioned above, the tetracyclic skeletons of **2a** and **3a** are mirror images of each other. However, **2a** has the methyl substituent at the bridgehead carbon next to the carbonyl group, whereas the **3a** has no bulky substituent at the corresponding position of mirror image. It is also found from the X-ray structure of **2a** that the relevant methyl group adopts a quasieclipsed conformation with the carbonyl group (dihedral angle of 28.9° for CH_3−C−C=O linkage). These steric circumstances may exert a significant interference against the approach of Lewis acid to the lone pair in a transoid fashion (with respect to the cyclopropane ring), resulting in the lower lability of cyclopropane

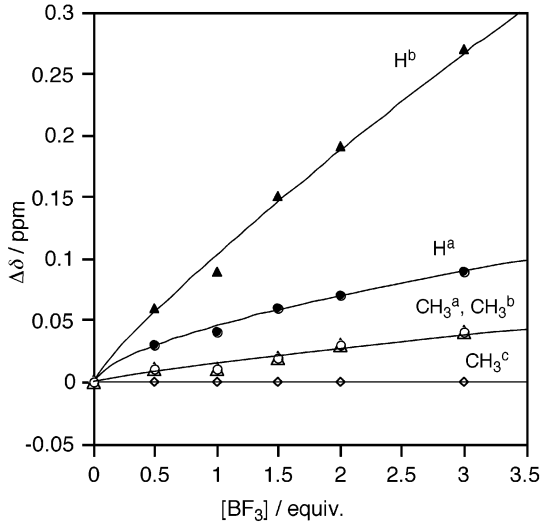

FIGURE 3. Plots of ^{1}H NMR differential chemical shifts ($\Delta\delta$) for **1a** (30 mM) with various equivalency of BF_3 in $CDCl_3$ at 25 °C. For each proton, see Chart 2. The values of $\Delta\delta$ ($= \delta_{BF3} - \delta_{none}$) and the chemical shifts (δ_{none}) of **1a** are available in the Supporting Information.

TABLE 3. PM3 Calculation of Heat of Formation (ΔH_f = kcal mol^{-1}) for Complexes of 1a−d with BF_3 and $AlCl_3$

		ΔH_f/kcal mol^{-1}				
substrate	acid	a_1	a_2	b_1	b_2	$\Delta\Delta H_f(a_1-b_2)$
1a	BF_3	−235.1	−232.2	−227.9	−232.2	−2.9
1a	$AlCl_3$	−79.0	−78.8	*b*	−79.8	0.8
1b	BF_3	−197.7	−197.8	−193.4	−199.4	1.7
1b	$AlCl_3$	−43.4	−42.6	*b*	−43.9	0.5
1c	BF_3	−273.0	−270.5	−269.7	−273.1	0.1
1c	$AlCl_3$	−118.9	−117.6	*b*	−119.1	0.2
1d	BF_3	−277.4	−275.0	−275.4	−279.9	2.5
1d	$AlCl_3$	−120.8	−120.8	*b*	−123.4	2.6

[a] Binding sites (a_1 − b_2) are the lone pair electrons to which Lewis acids bond (see Chart 2). [b] Converged to the b_2-bound structure even if started from $\mathbf{b}_1$ binding.

(10) Shambayati, S., Crowe, W. E., Schreiber, S. L. *Angew. Chem., Int. Ed. Engl.* **1990**, *29*, 256.

(11) We carried out the PM3 calculations only for BF_3 and $AlCl_3$ since these acids prefer to form the 1:1 complexes with carbonyl bases. By contrast, the complex structures of $SnCl_4$ and $TiCl_4$ are rather complicated because of their strong tendency to form the 2:1 complexes and the 1:1 dimeric complexes, satisfying the desire of Ti and Sn for hexacoordination; see ref 18.

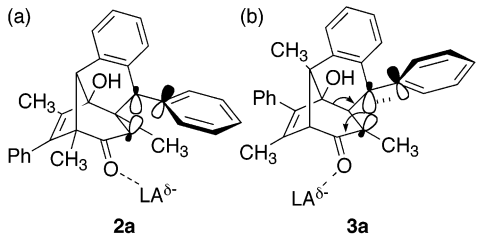

FIGURE 4. Schematic drawing of orbital interaction between the p-orbital of the *endo*-phenyl group and the breakable σ-bond of cyclopropane: (a) unfavorable twisted orientation for **2a** and (b) favorable parallel orientation for **3a**.

ring. This is not the case for **3a**, where the less hindered lone pair would accept Lewis acid in the transoid manner.[12] In addition, the *exo*-phenyl group as well as the bridged phenylene nucleus is expected to play an important role in the cyclopropane ring cleavage because the π-conjugation will accelerate the cyclopropane bond fission.[13] The present heterolytic cyclopropane ring cleavage promoted by Lewis acid complexation is most favorably performed in a conformation, in which the breaking bond is suitably oriented parallel to the component p-orbital of aromatic nuclei (Figure 4). Such a stereoelectronic requirement is intrinsically well attained in **3a** because the *exo*-phenyl ring is favorably twisted due to the vicinal steric hindrance with R^3 (= CH_3). However, **2a** cannot enjoy such a spatial orientation of *exo*-phenyl ring and rather adopts the orthogonal orientation of the relevant cyclopropane ring against the aromatic p-orbital. Incidentally, the phenylene bridge exerts almost the same conjugative affection on both **2a** and **3a** on account of the rigid bisected conformation with cyclopropane ring.[14]

The answer to the third question on the enantioselective formation of **4a**α is dependent on whether this compound is the kinetically or thermodynamically controlled product. The MOPAC PM3 calculation indicated that the **4a**α is less stable than the β-epimer by only 1.0 kcal mol^{-1} (Table 2). If the calculation is correct, the stereoselective proton transfer in the transformation **3a** → **4a**α should take place from the backside of the resulting sp^2 transition-state hybridized carbon (Chart 3a).[15] This assumption also requires the absence of keto−enol tautomerization. Otherwise, such an isomerization would necessarily provide the thermodynamically stable β-epimer likewise in the tautomerization of **5**α.

The last question (on the exclusive formation of less stable **5a**α) can be solved by assuming the proton transfer under the kinetically controlled condition as well as the subsequent $TiCl_4$-catalyzed tautomerization. Indeed, a prolonged treatment of **5a**α with $TiCl_4$ resulted in a

CHART 3

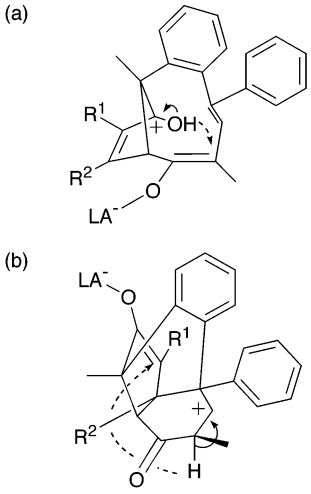

significant epimerization into the more stable **5a**β (Table 1, entries 5 and 6). Absence of such $\alpha \rightarrow \beta$ isomerization in case of other Lewis acids ($AlCl_3$, $SnCl_4$, and BF_3) may be due to the reduced acidity.[15] The formation of **5a**α can be ascribed to the Michael-type cyclization of **4a**α accompanied by a kinetically controlled proton transfer akin to the formation of **4a**α itself (Chart 3b).

Reaction of Diphenylacetylene Adduct 1b. To further explore the steric effects of alkyne substituents, we examined the Lewis acid catalyzed rearrangement of diphenylacetylene adduct **1b**. As shown in Table 1 (entries 7−12), the reaction of **1b** was considerably different from that of **1a** in several points.

(i) The reactivity of **1b** was relatively lower than that of **1a**.

(ii) **1b** showed only the path B route to give the isolable keto alcohol **3b**.

(iii) **3b** gradually rearranged to the epimeric mixture of **4b**α and β except for $TiCl_4$.

(iv) However, both α- and β-epimers did not undergo the Michael-type cyclization.

Points i and ii can be interpreted by the increased steric congestion at the lone pair electron a_1 by R^2 (= Ph), which would suppress the path A reaction (Scheme 1). As to point iii, the kinetic reason argued for the predominant formation of the **4a**α isomer must somewhat impede the proton transfer via a shortcut because of the disadvantageous steric and hydrophobic effects by substituent R^2 (= Ph). The reason for observation iv can be ascribed to the increased steric hindrance by the Ph substituent on intramolecular ring closure (Scheme 1). Instead, **4b** suffered the facile intramolecular [2 + 2] photocycloaddition.[16] Of great interest is that only the $TiCl_4$-catalyzed reaction could not cause the cyclopropane ring cleavage of keto alcohol **3b** even on extended standing for 200 h (entry 12). But, as expected, the addition of 3 equiv of BF_3 to the reaction solution awaked **3b** to revive the transformation into **4b**α and **4b**β (about 20% conversion of **3b** even on 1 h treatment). At present, we have no sophisticated explanation for this mysterious phenomenon, although the substituent R^2 (= Ph) is certainly

(12) The transoid binding may allow the favorable $\sigma^*-\sigma$ interaction between the coordination σ^* bond and the adjacent cyclopropane connecting σ-bond. Such an orbital interaction will intensify the electron demand of the relevant bond, which results in the promotion of the cyclopropane ring cleavage; see ref 7.

(13) (a) Rappoport, Z. *The Chemistry of the Cyclopropyl Group*; Wiley: New York, 1987; Vols. 1−2. (b) Wong, H. N. C.; Hon, M.-Y.; Tse, C.-W.; Yip, Y.-C. *Chem. Rev.* **1989**, *89*, 165.

(14) (a) Wilcox, C. F.; Loew, L. M.; Hoffmann, R. *J. Am. Chem. Soc.* **1973**, *95*, 8192. (b) Harmony, M. D.; Mathur, S. N.; Choe, J.-I.; Kattija-Ari, M.; Howard, A. E.; Staley, S. W. *J. Am. Chem. Soc.* **1981**, *103*, 2961. (c) Jason, M. E.; Gallucci, J. C.; Ibers, J. A. *Isr. J. Chem.* **1981**, *21*, 95.

(15) Childs, R. F.; Mulholland, D. L.; Nixon, A. *Can. J. Chem.* **1982**, *60*, 801.

(16) Incidentally, the isolated **4b**α was easily transformed into the intramolecular [2 + 2] photoadduct on irradiation with a 300 W high-pressure mercury lamp. Details will be described elsewhere.

responsible for such a strange anesthetic action against $TiCl_4$. Here, it should be remembered that $TiCl_4$ has a great tendency to form the 2:1 or 1:1 dimeric complex rather than the 1:1 one.[17] Such complexation would exert the more steric hindrance because of the octahedral coordination of Cl ligands. However, $SnCl_4$ brought about the appreciable transformation **3b** → **4b**α and **4b**β (entry 8), regardless of being bulkier than $TiCl_4$ and also having a tendency to form 2:1 complex.[17] This may be partly due to the observation that the average bond length (M−O) for complexation with a carbonyl group is longer in Sn−O (2.4 Å) than in Ti−O (2.14 Å).[10] Consequently, in the reaction with $TiCl_4$, there will be a greater steric hindrance when **3b** takes part in the octahedral complexation with $TiCl_4$. However, there is nothing comparable in the reaction with BF_3 and $AlCl_3$.

Reactions of 1-Hexyne Adduct 1c and 3-Hexyne Adduct 1d. The Lewis acid-catalyzed reaction of 1-hexyne adduct **1c** again showed both path A and B rearrangements to afford a modest amount of stable tetracyclic keto alcohol **2c** together with the major tricyclic dione **5c**α (via **3c** and then **4c**) on treatment with $SnCl_4$, BF_3, and $TiCl_4$ (Table 1, entries 13−16). As in the case of **1a**, only $TiCl_4$ brought about the epimerization **5c**α → **5c**β on elongation of reaction time (entry 16). It is noteworthy that the proportion of **2c** varied in the very narrow range (21 to 26%). This is very much contrast to the case of **1a** (6 to 42%).

Like **1a**, **1d** provided the increasing tendency of path B product in the order of $TiCl_4$ > $SnCl_4$ > BF_3 (entries 17−19). Interestingly, note that the tricyclic dione **5d**α did not isomerize to the possible epimer **5d**β even on about 4 days' treatment with $TiCl_4$. This may be partly due to the smallest differential energy between **5d**α and **5d**β ($\Delta\Delta H_f = 2.0$ kcal/mol), as compared with the corresponding larger values of 5−8 kcal/mol for the epimerism of **5a**−**c** (Table 2).

Effects of Alkyne Substituents and Lewis Acids on Path B/A Ratio. As discussed above, since the partitioning between path A and path B routes is represented by eq 2, it can be significantly affected by the substituents of alkyne component and the nature of Lewis acid (steric bulk, acidity, as well as complexation stoichiometry and structure). The present Lewis acids become bulky in the order of BF_3 < $AlCl_3$ < $TiCl_4$ < $SnCl_4$.[18] Therefore, the decreasing trend of path A proportion in this order is suggestive of some drift of Lewis acid binding site from the a_1 to the diagonal b_2 lone pair. This is due to the increased steric hindrance with the R^2 substituent (CH_3 for **1a** and Et for **1d**) (Figure 3).[19]

As a result, coupled with the Lewis acid binding behavior of **1a**−**d**, the relative stability of possible carbocations **I** and **II** or positively charged transition states would affect the partitioning ratio of path B/path A. In addition, we cannot ignore the important role of acidity of these Lewis acids, since the increasing acidity of Lewis acid virtually results in the more acceleration of the path B because of the stabilization of the tertiary carbocation intermediate **II** (Scheme 1).

Conclusions

In this paper, we have investigated the Lewis acid-catalyzed rearrangements of highly strained [2 + 2] photoadducts **1** of various diphenylhomobenzoquinone with acetylenes. The compounds **1** underwent the novel consecutive skeletal rearrangements. The involved major processes are (a) the branching Wagner−Meerwein 1,2-vinyl anion migration followed by the phenylene annulation giving tricyclic keto alcohols **2** and **3**, (b) the cyclopropane ring opening (only **3**) to afford bicyclic dione **4**α (together with **4**β for diphenylacetylene adduct), and then (c) the Michael-type intramolecular cyclization leading to tricyclic diones **5**α. The factors affecting mechanism and reactivity of these reactions were discussed on the basis of the substituents on the tricyclo-[5.2.0.$0^{3,5}$]non-8-ene-2,6-dione frame as well as the nature of the Lewis acids (steric bulk, acidity, and structure of complex). The Michael-type reaction yielded the less stable epimer **5**α after the kinetically controlled proton transfer. Consequently, it is concluded that the diverse knowledge and information obtained in the present reactions will provide useful insight into the understanding of the Lewis acid-catalyzed rearrangements of ring-strained carbonyl compounds.

Experimental Section

All melting points were not corrected. The ^{1}H NMR (270.05 MHz) and ^{13}C NMR (60.40 MHz) spectra were recorded in a $CDCl_3$ solution using TMS as internal standard. The light source for all photoexperiments was a 300 W high-pressure Hg lamp. The rearrangement products were isolated using an HPLC equipped with a chromato-integrator, UV detector, and pump.

Materials. All Lewis acids and alkynes were used as purchased. Cyclobutene-fused homobenzoquinones **1a**−**d** were synthesized by the [2 + 2] photocycloaddition of the corresponding homobenzoquinone with alkynes as previously described.[3]

General Procedure for the Lewis Acid-Catalyzed Reactions of 1. Liquid Lewis acids were added into a $CDCl_3$ solution (670 μL) of **1a** (8.36 mg, 0.02 mmol) in an NMR tube using a microsyringe (10 μL) at room temperature. For $AlCl_3$, a given amount was introduced into the $CHCl_3$ solution. The progress of reaction was monitored by ^{1}H NMR. After a period of requisite time, the reaction solution was transferred into a separate funnel, diluted with chloroform (10 mL), and then washed with water (3 mL × 3). The aqueous layer was extracted with chloroform (5 mL × 2). The combined organic layer was washed with water (3 mL × 3) and then dried over calcium chloride. After the evaporation of the solvent, the residue was submitted for ^{1}H NMR analysis to determine the product distribution. The residue was charged on a HPLC with a semifractionation column to give successfully the rearranged products with a methanol−water mixture as eluent. These compounds were purified by recrystallization from hexane−benzene, and the structures were deduced from the ^{1}H and ^{13}C NMR and IR spectra, and the structures of **3b**, **4b**α, **2c**, **5c**α, **5c**β, **2d**, and **5d**α were confirmed by X-ray crystallographic analysis. The analytical data and the crystal structures for **2a**, **4a**α, **5a**α, and **5a**β were described elsewhere.[4]

(17) The 2:1 or 1:1 dimeric complexation of $TiCl_4$ is well-known and confirmed in crystal structures of the complexes with ethyl acetate and ethyl anisate. For example, see: (a) Brun, L. *Acta Crystallogr.* **1966**, *20*, 739. (b) Bassi, I. W.; Calcaterra, M.; Intrito, R. *J. Organomet. Chem.* **1977**, *127*, 305.

(18) Carlson, R.; Lundstedt, T.; Nordahl, Å.; Prochazka, M. *Acta Chem. Scand.* **1986**, *B40*, 522.

(19) We are resorted on the Taft's steric parameters E_s; H ($E_s = 0$), CH_3 (−1.24), Et (−1.31), Bu (−1.63), and Ph (−3.79). See: Unger, S. H.; Hansch, C. *Prog. Phys. Org. Chem.* **1976**, *12*, 91.

(1*S,2*R**,9*S**,10*R**,13*R**,14*S**)-13-Hydroxy-10,12,14-trimethyl-2,11-diphenylpentacyclo[8.4.1.0^{2,14}.0^{3,8}.0^{9,13}]pentadeca-3(8),4,6,11-tetraen-15-one (2a):** mp 222−223 °C; colorless crystal (hexane−benzene); ^{1}H NMR ($CDCl_3$) δ 0.98 (s, 3H), 1.13 (s, 3H), 1.80 (s, 1H, br), 2.10 (s, 3H), 2.60 (s, 1H), 3.56 (s, 1H), 6.58 (d, 2H, J = 7.3 Hz), 7.05−7.18 (m, 7H), 7.24−7.64 (m, 5H); ^{13}C NMR ($CDCl_3$) δ 13.3, 15.2, 16.0, 41.5, 43.9, 51.6, 63.8, 67.2, 77.2, 126.0, 127.1, 127.4, 127.6, 128.1, 128.4, 128.5, 128.6, 129.0, 129.3, 130.9, 131.1, 131.2, 135.3, 138.0, 138.8, 140.8, 147.1, 202.7; IR (KBr) 3434 (br, OH), 1672 (C=O) cm^{-1}.

(2*S,6*R**,8*R**)-2,5,8-Trimethyl-4,10-diphenyltricyclo[9.4.0.0^{2,6}]pentadeca-1(15),4,9,11,13-pentaene-3,7-dione (4aα):** mp 222−223 °C; colorless crystal (hexane−benzene); ^{1}H NMR ($CDCl_3$) δ 0.91 (d, 3H, J = 6.6 Hz), 1.71 (s, 3H), 2.20 (s, 3H), 2.89 (dq, 1H, J = 8.9, 6.6 Hz), 3.64 (s, 1H), 6.55 (d, 1H, J = 8.9 Hz), 6.89−6.97 (m, 3H), 7.22−7.27 (m, 9H), 7.41 (td, 1H, J = 7.9, 1.3 Hz), 7.61 (d, 1H, J = 7.9 Hz); ^{13}C NMR ($CDCl_3$) δ 14.8, 17.7, 27.0, 47.2, 54.6, 71.8, 126.6, 127.6, 127.7, 128.1, 128.7, 128.8, 131.1, 136.8, 139.3, 139.9, 142.1, 142.5, 205.5, 207.4; IR (KBr) 1705 (C=O) cm^{-1}.

(2*S,4*S**,5*R**,6*R**,10*R**)-2,5,8-Trimethyl-4,10-diphenyltetracyclo[9.4.0.0^{2,6}.0^{5,10}]pentadeca-1(15),8,11,13-tetraene-3,7-dione (5aα):** colorless crystal; ^{1}H NMR ($CDCl_3$) δ 1.52 (s, 3H), 1.74 (s, 3H), 1.75 (d, 3H, J = 1.3 Hz), 2.79 (s, 1H), 3.68 (s, 1H), 6.07 (d, 1H, J = 7.9 Hz), 6.38−6.45 (m, 3H), 6.88 (q, 1H, J = 1.3 Hz, vinyl), 6.89−7.24 (m, 8H), 7.35 (td, 1H, J = 7.9, 1.3 Hz), 7.44 (dd, 1H, J = 7.9, 1.3 Hz); ^{13}C NMR ($CDCl_3$) δ 15.2, 17.1, 26.1, 50.4, 55.0, 56.8, 63.2, 65.9, 125.6, 125.7, 126.6, 127.2, 127.4, 127.7, 128.0, 128.3, 128.6, 129.9, 130.1, 131.3, 133.8, 134.7, 138.5, 140.0, 157.7, 196.1, 207.0; IR (KBr) 1742, 1653 (C=O) cm^{-1}.

(2*S,4*R**,5*R**,6*R**,10*R**)-2,5,8-Trimethyl-4,10-diphenyltetracyclo[9.4.0.0^{26}.0^{510}]pentadeca-1(15),8,11,13-tetraene-3,7-dione (5aβ):** mp 260−261 °C; colorless prisms (hexane−benzene); ^{1}H NMR ($CDCl_3$) δ 0.58 (s, 3H), 1.75 (s, 3H), 1.77 (d, 3H, J = 1.5 Hz), 2.99 (s, 1H), 4.44 (s, 1H), 6.52 (br, 2H, Ar), 7.04 (d, 1H, J = 7.6 Hz), 7.12−7.13 (m, 3H), 7.18 (t, 1H, J = 7.6 Hz), 7.24−7.27 (m, 2H, Ar + vinyl), 7.35 (d, 1H, J = 7.6 Hz), 7.39−7.51 (m, 5H); ^{13}C NMR ($CDCl_3$) δ 15.6, 16.9, 21.5, 49.3, 56.8, 57.4, 57.6, 62.2, 126.8, 126.9, 127.6, 127.7, 127.8, 128.0, 128.3, 129.6, 130.0, 131.0, 134.3, 135.6, 137.3, 140.0, 141.1, 154.7, 196.2, 211.6; IR (KBr) 1749, 1659 (C=O) cm^{-1}.

(1*S,2*R**,9*R**,10*S**,13*S**,14*S**)-13-Hydroxy-9,14-dimethyl-2,11,12-triphenylpentacyclo[8.4.1.0^{2,14}.0^{3,8}.0^{9,13}]pentadeca-3(8),4,6,11-tetraen-15-one (3b):** colorless prisms (hexane−benzene); ^{1}H NMR ($CDCl_3$) δ 1.15 (s, 3H), 1.87 (s, 3H), 1.93 (s, 1H, br), 2.45 (s, 1H), 3.55 (s, 1H), 6.93 (d, 1H, J = 7.8 Hz), 7.07−7.58 (m, 18H); ^{13}C NMR ($CDCl_3$) δ 18.3, 19.3, 38.4, 44.2, 48.1, 53.9, 75.3, 80.4, 126.2, 126.9, 127.3, 127.4, 127.6, 128.0, 128.1, 128.1, 128.7, 129.3, 130.4, 132.3, 134.7, 135.1, 135.6, 135.8, 136.8, 138.3, 148.2, 203.8; IR (KBr) 3433 (br, OH), 1671 (C=O) cm^{-1}.

(2*S,6*R**,8*R**)-2,8-Dimethyl-4,5,10-triphenyltricyclo[9.4.0.0^{2,6}]pentadeca-1(15),4,9,11,13-pentaene-3,7-dione (4bα):** mp 226−227 °C; colorless prisms (hexane−benzene); ^{1}H NMR ($CDCl_3$) δ 0.72 (d, 3H, J = 6.6 Hz), 1.82 (s, 3H), 2.42 (dq, 1H, J = 9.2, 6.6 Hz), 4.27 (s, 1H), 6.64 (d, 1H, J = 9.2 Hz), 6.07−6.74 (m, 2H), 6.93 (dd, 1H, J = 7.6, 1.3 Hz), 7.09−7.24 (m, 4H), 7.27−7.36 (m, 15H), 7.43 (td, 1H, J = 7.6, 1.3 Hz), 7.68 (d, 1H, J = 7.6 Hz); ^{13}C NMR ($CDCl_3$) δ 14.4, 27.3, 47.0, 54.7, 69.2, 125.7, 126.8, 127.6, 127.8, 127.9, 128.0, 128.2, 128.3, 128.7, 128.9, 129.2, 130.0, 130.9, 131.3, 131.5, 134.6, 137.0, 139.2, 139.8, 141.8, 142.5, 157.3, 205.8, 207.4; IR (KBr) 1706 (C=O) cm^{-1}.

(1*S,2*R**,9*S**,10*R**,13*R**,14*S**)-11-*n*-Butyl-13-hydroxy-10,14-dimethyl-2-phenylpentacyclo[8.4.1.0^{2,14}.0^{3,8}.0^{9,13}]pentadeca-3(8),4,6,11-tetraen-15-one (2c):** mp 188−189 °C; colorless prisms (hexane−benzene); ^{1}H NMR ($CDCl_3$) δ 0.91 (t, 3H, J = 7.3 Hz), 1.10 (d, 3H, J = 1.0 Hz), 1.26−1.49 (m, 6H), 1.56 (s, 3H), 1.71 (br, 1H), 1.93−2.10 (m, 1H), 2.41 (s, 1H), 3.43 (s, 1H), 6.36 (t, 1H, J = 1.7 Hz), 6.46 (d, 1H, J = 7.3 Hz), 7.04−7.24 (m, 5H), 7.34−7.41 (m, 3H), 7.44−7.45 (m, 2H); ^{13}C NMR ($CDCl_3$) δ 13.7, 14.0, 14.6, 22.5, 27.2, 29.3, 42.4, 44.0, 51.3, 63.4, 68.7, 84.4, 126.0, 127.3, 127.5, 128.3, 128.9, 129.7, 130.7, 131.0, 136.2, 138.2, 139.0, 149.0, 202.0; IR (KBr) 3421 (br, OH), 1671 (C=O) cm^{-1}.

(2*S,4*S**,5*R**,6*R**,10*R**)-4-*n*-Butyl-2,8-dimethyl-10-phenyltetracyclo[9.4.0.0^{2,6}.0^{5,10}]pentadeca-1(15),8,11,13-tetraene-3,7-dione (5cα):** mp 177−178 °C; colorless prisms (hexane−benzene); ^{1}H NMR ($CDCl_3$) δ 0.00−0.81 (m, 1H), 0.54 (t, 3H, J = 6.9 Hz), 0.64−1.01 (m, 5H), 1.26−1.57 (m, 2H), 1.67 (s, 3H), 1.73 (d, 3H, J = 1.3 Hz), 2.46 (dq, 1H, J = 6.3, 4.6 Hz), 2.79 (d, 1H, J = 4.6 Hz), 3.32 (dd, 1H, J = 6.6, 4.6 Hz), 7.08 (d, 1H, J = 1.3 Hz), 7.18−7.33 (m, 7H), 7.52 (d, 2H, J = 1.3 Hz); ^{13}C NMR ($CDCl_3$) δ 13.7, 17.6, 22.7, 27.9, 30.2, 49.3, 50.7, 54.8, 56.5, 56.8, 127.0, 127.2, 128.1, 129.2, 129.5, 133.9, 135.3, 137.2, 144.5, 159.0, 196.6, 210.5; IR (KBr) 1741, 1666 (C=O) cm^{-1}.

(2*S,4*R**,5*R**,6*R**,10*R**)-4-*n*-Butyl-2,8-dimethyl-10-phenyltetracyclo[9.4.0.0^{2,6}.0^{5,10}]pentadeca-1(15),8,11,13-tetraene-3,7-dione (5cβ):** mp 207−208 °C; colorless prisms (hexane−benzene); ^{1}H NMR ($CDCl_3$) δ 0.56 (t, 3H, J = 7.2 Hz), 0.72−0.92 (m, 5H), 1.03−1.16 (m, 1H), 1.42 (t, 1H, J = 7.2 Hz), 1.63 (s, 3H), 1.79 (d, 3H, J = 1.3 Hz), 2.47 (dd, 1H, J = 10.9, 3.6 Hz), 2.63 (d, 1H, J = 4.9 Hz), 2.89 (d, 1H, J = 4.9 Hz), 7.09−7.24 (m, 3H), 7.27−7.43 (m, 7H); ^{13}C NMR ($CDCl_3$) δ 13.8, 15.8, 17.1, 21.7, 29.2, 29.6, 47.6, 51.1, 51.7, 53.9, 55.7, 126.9, 127.2, 127.7, 127.8, 128.3, 128.4, 129.6, 134.8, 137.2, 138.8, 143.2, 156.1, 196.8, 212.8; IR (KBr) 1741, 1665 (C=O) cm^{-1}.

(1*S,2*R**,9*S**,10*R**,13*R**,14*S**)-11,12-Diethyl-13-Hydroxy-10,14-dimethyl-2-phenylpentacyclo[8.4.1.0^{2,14}.0^{3,8}.0^{9,13}]-pentadeca-3(8),4,6,11-tetraen-15-one (2d):** mp 209−210 °C; colorless prisms (hexane−benzene); ^{1}H NMR ($CDCl_3$) δ 0.97 (t, 3H, J = 7.6 Hz), 1.06 (s, 3H), 1.12 (s, 3H), 1.19 (t, 3H, J = 7.6 Hz), 2.11−2.19 (m, 2H), 2.35−2.55 (m, 3H), 3.33 (s, 1H), 6.53 (d, 1H, J = 7.6 Hz), 7.04−7.15 (m, 4H), 7.32−7.43 (m, 3H), 7.45 (dd, 2H, J = 3.6, 1.3 Hz); ^{13}C NMR ($CDCl_3$) δ 11.5, 15.0, 19.9, 38.9, 43.5, 48.1, 63.0, 68.5, 75.8, 76.5, 77.0, 77.4, 125.9, 127.0, 127.4, 127.6, 127.7, 127.9, 128.1, 128.3, 129.3, 130.0, 130.2, 131.3, 132.3, 135.2, 137.0, 138.2, 139.1, 147.1, 205.0; IR (KBr) 3410 (br, OH), 1671 (C=O) cm^{-1}.

(2*S,4*S**,5*R**,6*R**,10*R**)-4,5-Diethyl-2,8-dimethyl-10-phenyltetracyclo[9.4.0.0^{2,6}.0^{5,10}]pentadeca-1(15),8,11,13-tetraene-3,7-dione (5dα):** mp 211−212 °C; colorless prisms (hexane−benzene); ^{1}H NMR ($CDCl_3$) δ 0.75 (t, 3H, J = 7.3 Hz), 0.83 (t, 3H, J = 7.3 Hz), 0.86−0.97 (m, 1H), 1.45−1.71 (m, 2H), 1.67 (s, 3H), 1.70 (d, 3H, J = 1.2 Hz), 2.03−2.10 (m, 1H), 2.30 (dd, 1H, J = 8.6, 3.6 Hz), 2.80 (s, 1H), 7.00 (dd, 1H, J = 7.6, 1.2 Hz), 7.06 (d, 1H, J = 1.2 Hz), 7.10 (td, 1H, J = 7.6, 1.2 Hz), 7.21−7.29 (m, 4H), 7.32−7.42 (m, 3H), 7.43−7.49 (m, 2H); ^{13}C NMR ($CDCl_3$) δ 8.02, 15.2, 15.2, 17.6, 21.0, 24.4, 52.0, 55.3, 56.7, 58.6, 126.3, 126.4, 127.0, 127.2, 127.3, 128.0, 129.3, 131.9, 132.6, 133.7, 134.7, 140.6, 140.7, 158.0, 195.7, 211.0; IR (KBr) 1740, 1660 (C=O) cm^{-1}.

X-ray crystal structure determination of 1a: $C_{30}H_{26}O_2$, M = 418.53, monoclinic, space group $P2_1/n$ with a = 13.3309(1) Å, b = 9.4105(1) Å, c = 18.7703(4) Å, β = 104.229(4)°, V = 2282.51(7) Å^3, Z = 4, D_c = 1.218 g/cm^3, R = 0.126, and R_w = 0.210 for 4181 reflections with $I > 0.0\sigma(I)$. Data were collected on a Rigaku RAXIS-RAPID imaging plate diffractometer with graphite monochromated Mo Kα radiation at room temperature. The number of variables was 393. The structure was solved by direct methods (SIR-92) and refined on F^2 by full-matrix least-squares methods.

X-ray crystal structure determination of 3b: $C_{40}H_{40}O_3$, M = 586.78, monoclinic, space group $P2_1/a$ with a = 30.28(1) Å, b = 9.475(7) Å, c = 11.233(6) Å, β = 93.86(4)°, V = 3125(3) Å^3, Z = 4, D_c = 1.176 g/cm^3, R = 0.083, and R_w = 0.095 for 4065 reflections with $I > 2.0\sigma(I)$. Data were collected on a Mac Science MXC3 diffractometer using graphite-monochromated Mo Kα radiation at room temperature. The number of vari-

ables was 500. The structure was solved by direct methods (SIR-92) and refined on F^2 by full-matrix least-squares methods.

X-ray crystal structure determination of 4bα: $C_{35}H_{28}O_2$, $M = 480.60$, monoclinic, space group $P2_1/n$ with $a = 10.267(3)$ Å, $b = 7.706(2)$ Å, $c = 32.75(2)$ Å, $\beta = 90.48(4)°$, $V = 2590(1)$ Å^3, $Z = 4$, $D_c = 1.232$ g/cm^3, $R = 0.070$, and $R_w = 0.055$ for 2450 reflections with $I > 3.0\sigma(I)$. Data were collected on a Rigaku RAXIS-II imaging plate diffractometer with graphite-monochromated Mo Kα radiation at room temperature. The number of variables was 334. The structure was solved by direct methods (SHELX-86) and refined on F^2 by full-matrix least-squares methods.

X-ray crystal structure determination of 2c: $C_{27}H_{28}O_2$, $M = 384.52$, monoclinic, space group $P2_1/c$ with $a = 8.7324(2)$ Å, $b = 12.0297(1)$ Å, $c = 19.8786(7)$ Å, $\beta = 97.193(4)°$, $V = 2071.77(1)$ Å^3, $Z = 4$, $D_c = 1.233$ g/cm^3, $R = 0.162$, and $R_w = 0.173$ for 4696 reflections with $I > 2.0\sigma(I)$. Data were collected on a Rigaku RAXIS-RAPID imaging plate diffractometer with graphite-monochromated Mo Kα radiation at room temperature. The number of variables was 262. The structure was solved by direct methods (SIR-92) and refined on F^2 by full-matrix least-squares methods.

X-ray crystal structure determination of 5cα: $C_{27}H_{28}O_2$, $M = 384.52$, trigonal, space group R-3 with $a = 37.811(3)$ Å, $c = 8.1627(7)$ Å, $V = 10106.4(13)$ Å^3, $Z = 18$, $D_c = 1.137$ g/cm^3, $R = 0.071$, and $R_w = 0.094$ for 2883 reflections with $I > 3.0\sigma(I)$. Data were collected on a Rigaku Mercury detecter with graphite-monochromated Mo Kα radiation at room temperature. The number of variables was 291. The structure was solved by direct method (SAPI-91) and refined on F^2 by full-matrix least-squares methods.

X-ray crystal structure determination of 5cβ: $C_{27}H_{28}O_2$, $M = 384.52$, monoclinic, space group $C2/c$ with $a = 25.590(13)$ Å, $b = 8.664(4)$ Å, $c = 22.215(11)$ Å, $\beta = 118.790(7)°$, $V = 4316.3(32)$ Å^3, $Z = 8$, $D_c = 1.183$ g/cm^3, $R = 0.149$, and $R_w = 0.199$ for 4805 reflections with $I > -10.00\sigma(I)$. Data were collected on a Rigaku Mercury detecter with graphite-monochromated Mo Kα radiation at room temperature. The number of variables was 290. The structure was solved by direct methods (SIR-92) and refined on F^2 by full-matrix least-squares methods.

X-ray crystal structure determination of 2d: $C_{27}H_{28}O_2$, $M = 384.52$, monoclinic, space group $P2_1/a$ with $a = 13.085(2)$ Å, $b = 8.907(2)$ Å, $c = 18.254(3)$ Å, $\beta = 95.486(5)°$, $V = 2117.9(2)$ Å^3, $Z = 4$, $D_c = 1.206$ g/cm^3, $R = 0.144$, and $R_w = 0.162$ for 4805 reflections with $I > 2.0\sigma(I)$. Data were collected on a Rigaku RAXIS-RAPID imaging plate diffractometer with graphite-monochromated Mo Kα radiation at room temperature. The number of variables was 262. The structure was solved by direct methods (SIR-92) and refined on F^2 by full-matrix least-squares methods.

X-ray crystal structure determination of 5dα: $C_{27}H_{28}O_2$, $M = 384.52$, triclinic, space group P-1 with $a = 14.080(2)$ Å, $b = 18.049(1)$ Å, $c = 10.0850(9)$ Å, $\alpha = 104.981(4)°$, $\beta = 108.503(6)°$, $\gamma = 109.737(3)°$, $V = 2086.9(4)$ Å^3, $Z = 4$, $D_c = 1.224$ g/cm^3, $R = 0.233$, and $R_w = 0.265$ for 9028 reflections with $I > 2.0\sigma(I)$. Data were collected on a Rigaku RAXIS-RAPID imaging plate diffractometer with graphite-monochromated Mo Kα radiation at room temperature. The number of variables was 579. The structure was solved by direct methods (SIR-92) and refined on F^2 by full-matrix least-squares methods.

Crystallographic data (excluding structure factors) for the structures in this paper have been deposited with the Cambridge Crystallographic Data Centre as supplementary publication numbers CCDC 162122-162125 (for **2a**, **4a**α, **5a**α and **5a**β), 224913−224919 (for **3b**, **4b**α, **2c**, **5c**α, **5c**β, **2d**, **5d**α) and 225163 (for **1a**).

Acknowledgment. We gratefully appreciate financial support by General Sekiyu Research & Development Encouragement & Assistance Foundation. This work was also supported by a Grant-in-Aid for Scientific Research on Priority Areas (No.10650849) from the Ministry of Education, Culture, Sports, Science and Technology of the Japanese Government. We are grateful to Dr. T. Kawamoto (Osaka University) for measurement of X-ray analysis for **3b** and **5a**α.

Supporting Information Available: CIF files and ORTEP drawings of **1a**, **2a**, **4a**α, **5a**α, **5a**β, **3b**, **4b**α, **2c**, **5c**α, **5c**β, **2d**, and **5d**α, and a table of the ^{1}H NMR differential chemical shifts ($\Delta\delta$) for the complexation of **1a** with BF_3. This material is available free of charge via the Internet at http://pubs.acs.org.

JO035830K